frontiers in Physics

BRIEF RESEARCH REPORT
published: 20 August 2021
doi: 10.3389/fphy.2021.720539

Faster-Than-Nyquist 400 G Implementation Using 126-GBaud QPSK-OFDM With 88-GSa/s Undersampling

Peng Liu[1], *Hongxian Chen*[2], *Weihao Ni*[3] *and Fan Li*[3]*

[1]The School of Computer, Guangdong University of Technology, Guangzhou, China, [2]PLA Troops, Guangzhou, China, [3]The Key Laboratory of Optoelectronic Materials, School of Electronics and Information Technology, Sun Yat-Sen University, Guangzhou, China

In this study, we demonstrated generation and transmission of 114 Gbaud and 126 Gbaud faster-than-Nyquist (FTN) discrete Fourier transform-spread (DFT-spread) quadrature phase shift keying orthogonal frequency division multiplexing (QPSK-OFDM) with 88-Gsa/s sampling rate digital-to-analog converters (DACs) experimentally. It is the first time to realize 400G FTN DFT-spread QPSK-OFDM signal per optical carrier for metro and regional applications, which will be a solution for network operators to address the issue of increasing bandwidth derived from the rapid popularization of mobile Internet and the wide application of IoT (Internet of Things technology). Delay-and-add filter (DAF) is adopted to realize frequency shaping at the transmitter to keep higher portions of energy of signal at low frequencies, which makes the OFDM much more robust to strong filtering effect. After pre-equalization, bit error rate (BER) performance of 114 GBaud and 126 GBaud FTN DFT-spread QPSK-OFDM has been significantly improved, and maximum-likelihood sequence estimation (MLSE) shows a better effect than binary decoding in the aspect of against the inter symbol interference (ISI) introduced by spectrum compression. The effective bit rate of dual polarization 126 Gbaud FTN DFT-spread QPSK-OFDM which is generated with 88 GSa/s sampling rate is 410.08 Gb/s, to the exclusion of all overhead including TSs, cyclic prefix (CP), and 20% forward error correction (FEC) coding. We successfully transmit 8 × 400 Gbit/s FTN DFT-spread QPSK-OFDM signal generated from 88 Gsa/s sampling rate DAC over 420 km single mode fiber (SMF) with the BER under 2.4×10^{-2}.

Keywords: orthogonal frequency division multiplexing, discrete fourier transform-spread, WDM, pre-equalization, faster-than-nyquist

OPEN ACCESS

Edited by:
Qiang Xu,
Nanyang Technological University, Singapore

Reviewed by:
Jia Lu,
Hebei University of Technology, China
Zhou Hui,
Hunan Normal University, China

***Correspondence:**
Fan Li
lifan39@mail.sysu.edu.cn

Specialty section:
This article was submitted to Optics and Photonics, a section of the journal Frontiers in Physics

Received: *04 June 2021*
Accepted: *12 July 2021*
Published: *20 August 2021*

Citation:
Liu P, Chen H, Ni W and Li F (2021) Faster-Than-Nyquist 400 G Implementation Using 126-GBaud QPSK-OFDM With 88-GSa/s Undersampling. Front. Phys. 9:720539. doi: 10.3389/fphy.2021.720539

INTRODUCTION

Faster-than-Nyquist (FTN) is extensively studied to improve the spectrum efficiency by transmitting symbols within a bandwidth less than the Nyquist bandwidth [1–9]. This technique has been put forward and performed in 400G single-carrier coherent optical transmission systems recently [10]. Faster-than-Nyquist root-raised cosine (FTN-RRC) filter has been proposed to generate sub-symbol-rate sampling signal. 483 Gb/s (120.75 Gbaud) single-carrier polarization-division-multiplexed quadrature phase-shift keying (PDM-QPSK) signal is demonstrated by using a 92 GSa/s

digital-to-analog convertor (DAC) with sampling rate 0.76 sample/symbol. We consider that transmission of higher order quadrature amplitude modulation (QAM) signal is a method to effectively improve spectrum efficiency, however, the optical signal-to-noise ratio (OSNR) and stringent system linearity requirements prevent the transmission of high-order QAM modulated signal from optical fiber communication system. Compared to high-order QAM modulated signal transmission, there are following advantages to enhance spectral efficiency with FTN techniques. First, low-order modulation formats with a relatively high spectrum compression factor that can effectively solve the system linearity requirement problem. Second, we can set the signal compression ratio flexibly within the maximum compression ratio in our experiment, which can better approach the theoretical maximum transmission capacity of the channel.

FTN orthogonal frequency division multiplexing (OFDM) is first reported in Ref. [11] with discrete Fourier transform-spread (DFT-spread) and duo-binary spectrum shaping techniques. In the DFT-spread technique, using all in-band subcarriers delivers each data symbol [12, 13]. The single carrier–alike characteristic of DFT-spread OFDM signals show much better filtering effect tolerance than conventional OFDM signals. In addition, digital delay addition filter (DAF) is used to perform spectrum shaping to further improve the filtering effect tolerance [6]. In Ref. [11], as several sub-bands are applied to transmit signal, inter-sub-band interference (ISBI) appears in multi-band FTN OFDM, complicated digital signal processing (DSP) algorithms is necessary to compensate ISBI. Also, it is still questionable whether it could be a potential option to its single-carrier counterpart delivering 400G services per wavelength for metro and regional applications, which requires further investigation. Recently we have succeeded in transmitting the highest equivalent baud rate (120 Gbaud) FTN DFT-spread QPSK-OFDM signal within 80 GHz channel bandwidth over 80 km SMF with the BER under SD-FEC limitation of 2.4×10^{-2}. We make use of 80 GSa/s sampling rate to generate dual polarization 120 Gbaud FTN DFT-spread QPSK-OFDM and the pay-load bit rate is 384.54 Gb/s excluding all overhead including TSs, cyclic prefix (CP), and 20% FEC coding. In order to further improve the spectral efficiency, we integrated wavelength division multiplexing (WDM) system with FTN DFT-spread system, and increased the single-channel pay-load bit rate to more than 400G by using 88 Gsa/s sampling rate DACs.

In this study, generation and transmission of 400G FTN QPSK-OFDM signal are experimentally demonstrated with single DFT-spread band to avoid multi-band ISBI. To achieve a symbol rate higher than the Nyquist bandwidth, spectral of single-band DFT spread is compressed and ISBI cancellation technique is avoided in the receiver. Maximum likelihood sequence estimation (MLSE) decoding [6, 14] and pre-equalization [15, 16] are implemented to compensate inter symbol interference (ISI) caused by insufficient bandwidth and spectral compression, which can improve the receiver sensitivity significantly. We generate and transmit a record high baud rate (126 Gbaud) QPSK-OFDM signal with 88 GSa/s Sampling rate DAC. Finally, 8 × 400 Gb/s WDM FTN QPSK-OFDM with 22.8% spectral compression ratio within 100 GHz grid are successfully transmitted over 420-km with the BER under soft-decision FEC (SD-FEC) threshold (2.4×10^{-2}).

PRINCIPLE

Compared to the scheme proposed in Ref. [11], only one sub-band is discussed in this article, and ISBI between sub-channels is avoided. Directly subcarriers discarding at high frequencies instead of spectrum overlapping are applied to achieve symbol rate higher than the Nyquist bandwidth. After duo-binary DAF encoding, the signal becomes a cosine-alike spectrum shape. Because the serious ISI of high-frequency subcarriers will be induced when the channel bandwidth less than signal baud rate, transmitting a conventional OFDM signal *via* this channel is not practical. For DFT-spread OFDM signal, each QPSK symbol is carried on all data-carried subcarriers when single-band DFT spread is realized. In the circumstances, serious ISI on high-frequency subcarriers are spread over all symbols equally and still lead to BER performance deterioration. In FTN DFT-spread OFDM scheme, duo-binary encoding is realized by differential encoding and DAF. Compared to DFT-spread OFDM, FTN DFT-spread OFDM shows better performance in overcoming severe ISI, as the cosine-alike shape spectral density of FTN DFT-spread OFDM signal is much more robust to strong brick-wall filtering effect.

Principle diagram for FTN DFT-spread QPSK-OFDM generation is described in our previous work in detail [17], QPSK samples are divided into in-phase/quadrature (I/Q) branches and then fed into duo-binary encoding. With differential encoding, the symbols can be easily demodulated [18, 19], or else the symbols should be demodulated with MLSE for nine-level quadrature amplitude modulation (9QAM) [6, 11]. MLSE takes advantage of duo-binary memorability between adjacent codes to select the largest possible path to minimize BER and to further reduce ISI and noise. In this study, the transmitted symbols of FTN DFT-spread OFDM signal are duo/poly-binary encoded in the transmitter. In the DAF, the memory length is only one symbol, which coincides with the algorithm idea of MLSE. In the receiver, we can make use of the inherent memory length of symbols to minimize the BER by MLSE decoding. In addition, since the memory length of symbols is only 1, using MLSE algorithm is not computationally difficult. For QPSK and M-QAM modulation schemes, we usually divide them into in-phase and orthogonal components. In this way, the signals of the two components are in the M-level pulse amplitude modulation (M-PAM) format. Therefore, the following algorithm introduction is based on M-PAM modulation. **Figure 1A** shows the duo-binary signal frame diagram of M-PAM (where M = 2 and 4). **Figure 1C** and **Figure 1D** display the spectra of 4-PAM signal before and after through duo-binary process, respectively. Generally, the transmission process of a binary channel can be explained by a finite state machine. The state transition frame diagram is used to represent this state machine, where $x(n)$ represents the states at the moment n, when M = 2,

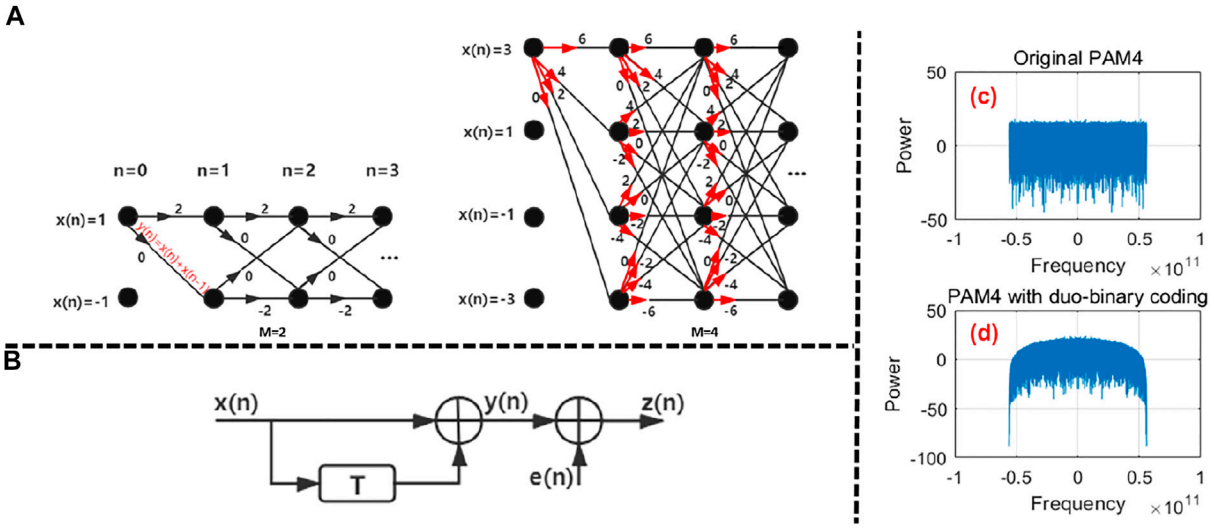

FIGURE 1 | (A) Duo-binary signal frame diagram of M-PAM, **(B)** simplified channel model of Duo-binary pulse shaping, **(C)** spectrum of 4-PAM signal, and **(D)** spectrum of duo-binary 4-PAM signal.

$x(n) \in \{1, -1\}$ and when M = 4, $x(n) \in \{3, 1, -1, -3\}$.$x(1)$ is the input at the first time. And $x(n) + x(n\text{-}1)$ which is attached to the branch stands for the transition of states between moment n-1 and n.

As can be seen from equation $y(n) = x(n) + x(n-1)$, it is obvious that the input of the node $y(1)$ is needed for the output $x(0)$ at the first moment, and we can take any value in $x(0) \in \{1, -1\}$ because the influence of the selection of the initial state on the MLSE algorithm in the long-distance transmission is negligible. The marked value of the line between nodes at two adjacent moments in the figure is determined by $y(n) = x(n) + x(n-1)$. It can be found that any node has M conversion possibilities, and from the moment $n = 2$, each node has M possible input paths. In order to more intuitively explain the implementation principle of MLSE, we simplified the duo-binary channel model as shown in **Figure 1B**.

$z(n)$ and $e(n)$ represent the sampling value of the received signal and the sampling value of the noise at the moment n, respectively, and T represents the delay of a sign time. The basic idea of the MLSE algorithm is to find the most likely path that maximizes the conditional probability of $P(Z(n)|X(n))$, where $Z(n) = [z(1), z(2), \ldots, z(n)]$ is the vector representation of the sampled value of the received signal and $X(n) = [x(1), x(2), \ldots, x(n)]$ is the vector representation of the input signal. We define $Y(n) = [y(1), y(2), \ldots, y(n)]$ to be an ideal vector representation of the output signal. It can be seen from formula $y(n) = x(n) + x(n-1)$ that $y(n)$ is uniquely determined by $x(n)$, so the maximum value of conditional probability $P(Z(n)|X(n))$ can be converted into the maximum value of conditional probability $P(Z(n)|Y(n))$, that is, the minimum value of Euclidean distance $D(Z(n), Y(n))_{\min}$ between vector $Y(n)$ and $Z(n)$. Based on the definition of Euclidean distance, it can be expressed as the sum of independent one-dimensional variables as follows:

$$D(Z(n), Y(n)) = \sum_n (z(n) - y(n))^2 = \sum_n [z(n) - (x(n) + x(n-1))]^2. \quad (1)$$

For the Euclidean distance $DM(x(1))$ between node $x(1)$ at the first receiver-side and the initial node $x(0)$, where $x(1)$ has M values, at the moment $n = 1$, each different node has corresponding Euclidean distance $DM(x(1))$ with sampling received signal $z(1)$ so $DM(x(1))$ has M values.

As shown in **Figure 1A** from the moment $n = 2$, each node $x(n)$ has M input paths and M different values of $x(n)$. So for every moment n, M^2Euclidean distance $DM(x(n))$ can be calculated by the Euclidean distance at the current time and the Euclidean distance that we calculated before. The maximum of conditional probability $P(Z(n)|Y(n))$ at the moment n can be converted to finding time n of $D(Z(n), Y(n))_{\min}$. For a specific $x(n)$ of one of M values at the moment n, the minimum value of M Euclidean distances can be used as $DM(x(n))$ of the current node, and $DM(x(n))$ can be defined as follows:

$$DM(x(n)) = \min \{DM(x(n-1)) + [z(n) - (x(n) + x(n-1))]^2\}. \quad (2)$$

It can be seen that for the specific input path $x(n)$ at the moment n, which originally had M different input paths, only one surviving path would be left through the above formula, and the other M-1 paths would be discarded to reduce the storage capacity required by the algorithm. However, in the actual MLSE algorithm, the input sequence is often very long. It is not possible to store a minimum Euclidean distance for each time node. Therefore, the common processing method is to truncate the signal once after the time of K symbols. In this way,

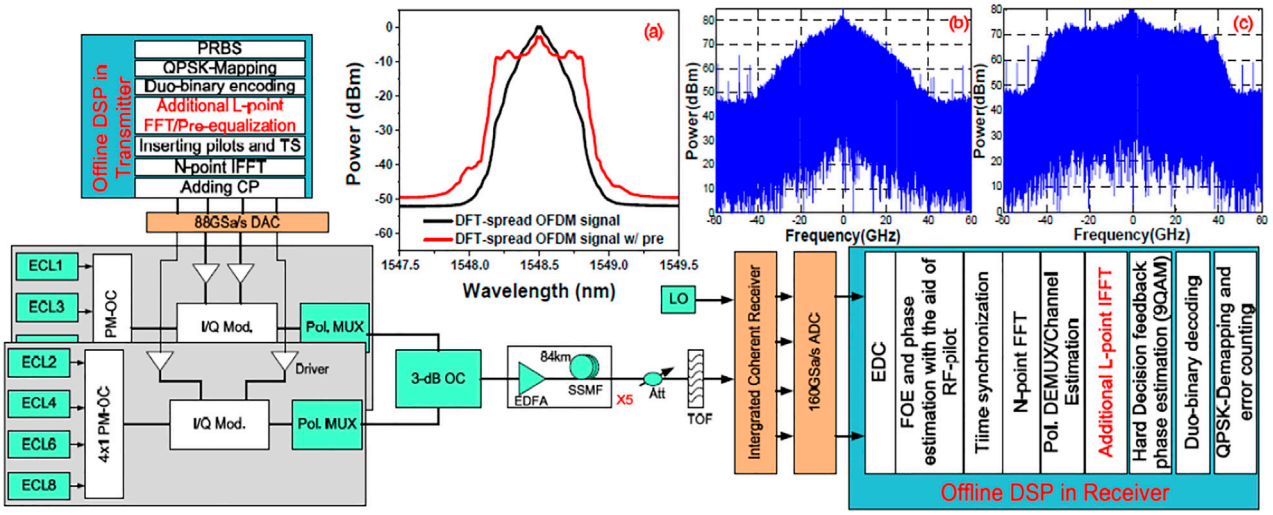

FIGURE 2 | Experimental setup (ECL: external cavity lasers; DAC: time-division Multiplexer; I/Q Mod.: IQ modulator; Pol. MUX: polarization multiplexer; OC: optical coupler; ATT: attenuator; TOF: tunable optical filter; LO: local oscillator; ADC: analog-to-digital convertor). Insets: **(A)** 114 Gbaud FTN-QPSK-OFDM optical spectrum, 114 Gbaud FTN-QPSK-OFDM electrical spectrum **(B)** without and **(C)** with pre-equalization.

we only need to store M viable paths within K symbols, which greatly reduces the load of memory. However, the value of K often has a great impact on the performance of MLSE algorithm. First of all, K must be greater than the memory length of the symbol, otherwise the Euclidean distance calculated and survived may not be the minimum value. Moreover, if the value of K is too large, the consistency of memory will be increased. For double/multiple binary signals with a memory length of one for M = 2 and 4, the performance penalty for MLSE is almost negligible when the K value is above 20.

EXPERIMENTAL SETUP AND RESULTS

The experimental setup for 8 × 400 Gbit/s FTN-DFT-spread QPSK-OFDM signal generation, transmission, and reception is shown in **Figure 2**. In the transmitter, we use 8 100-GHz channel spacing external cavity lasers (ECLs) with <100-kHz linewidth and 14.5 dBm output power as the light sources in the transmitter. They are divided into two groups as the odd and even channels to form the WDM channel setup in 100 GHz-grid. The odd and even channels are combined with two sets of polarization multiplexer optical couplers (PM-OCs). FTN QPSK-OFDM is generated with MATLAB as described above and then uploaded into an 88 Gsa/s sampling rate DAC and the 3-dB bandwidth of the DAC is 16 GHz. The 3-dB bandwidth of driver and optical modulator are 30 GHz and 25 GHz, respectively. The odd and even channels I/Q modulators biased at null point are independently modulated by the four output ports of the DAC. We employ the polarization multiplexer to realize the polarization multiplexing of the signal [20], in our experiment, the even and odd channels are combined by a 2 × 1 optical coupler (OC). We can take advantage of

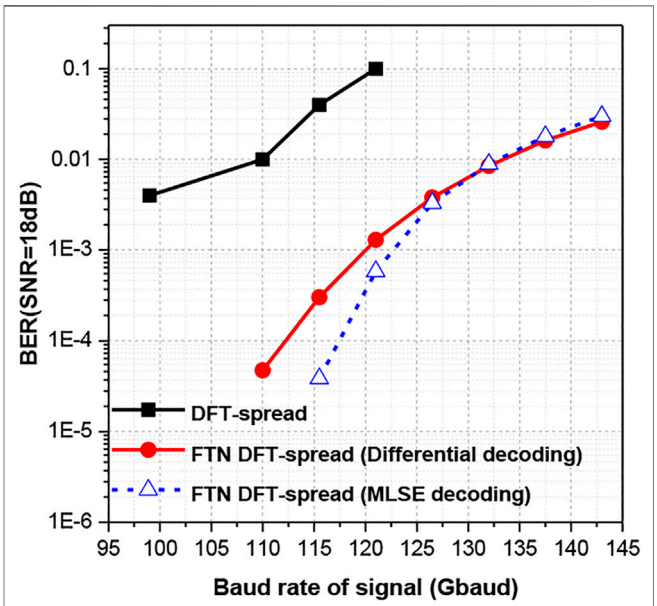

FIGURE 3 | BER versus baud rate of FTN-DFT-spread QPSK-OFDM in AWGN channel.

effective OFDM signal baud rate **B** to adjust the DFT-spread fast Fourier transform/inverse fast Fourier transform (FFT/IFFT) size ***M***. The relationship between them can be expressed as: $\boldsymbol{M} = (\boldsymbol{N} \times \boldsymbol{B})/\boldsymbol{88}$. Among the $\boldsymbol{N}$ = 1,024 subcarriers. The first subcarrier of FTN DFT-spread signal is reserved null for direct-current bias (DC-bias). As frequency offset estimation (FOE) and phase noise estimation is realized with radio frequency pilot (RF-pilot) scheme [17], another five subcarriers around zero frequency are reserved for RF-pilot insertion, and the rest $\boldsymbol{L}$ ($\boldsymbol{L} = \boldsymbol{N}$-$\boldsymbol{6}$)

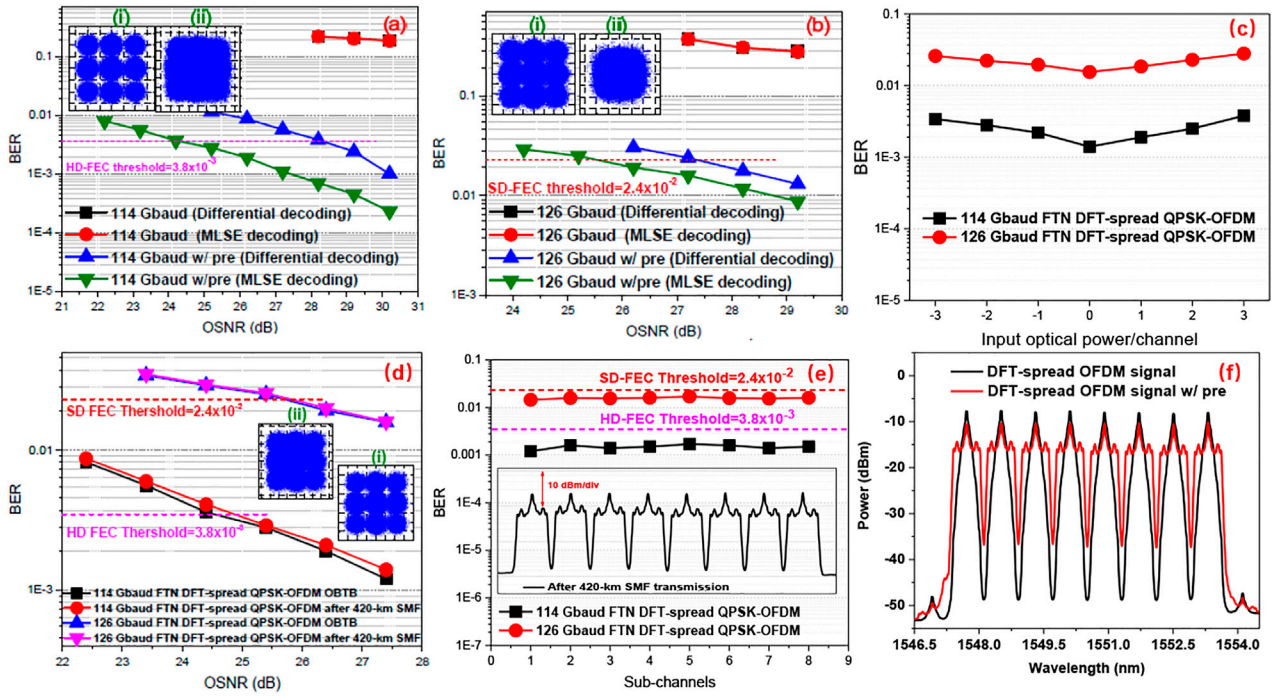

FIGURE 4 | (A) BER versus OSNR of 114 Gbaud FTN-DFT-spread QPSK-OFDM after 420-km fiber transmission, **(B)** BER versus OSNR of 126 Gbaud FTN-DFT-spread QPSK-OFDM after 420-km fiber transmission. BER versus OSNR of the 3rd sub-channel of WDM in OBTB and after 420-km fiber transmission, **(C)** BER versus input power per channel of the 3rd sub-channel of WDM after 420-km transmission, **(D)** BER versus OSNR of the 3rd sub-channel of WDM in OBTB and after 420-km fiber transmission, **(E)** BERs versus all sub-channels of 114 and 126 Gbaud FTN-DFT-spread QPSK-OFDM after 420-km fiber transmission, and **(F)** optical spectrum (0.02 nm) of WDM signal after 420-km fiber transmission.

subcarriers excluding above-mention six subcarriers are adopted to carry FTN DFT-spread QPSK symbols. The length of CP is eight sample and a pair of training symbols (TSs) is inserted between every 123 OFDM symbols for synchronization and channel estimation. The modulated signal is launched into five spans of 84-km SMF link. There are 18-dB average loss and 17.5-ps/km/nm chromatic dispersion (CD) at 1,550 nm in each span. An erbium doped fiber amplifier (EDFA) is used before each span to compensate for the fiber loss. At the receiver, an ECL with linewidth <100 kHz is used as a local oscillator (LO). We use an integrated coherent receiver (ICR) to achieve the O/E detection. The signal is captured by a 160 GSa/s sampling rate real-time oscilloscope and then processed with offline DSP shown in **Figure 2**.

Figure 3 gives out the simulation results of 99–143 GBaud DFT-spread QPSK-OFDM signal, in which FTN DFT-spread QPSK-OFDM signal is generated with 88 Gsa/s sampling rate DAC and an additive white Gaussian noise (AWGN) channel with signal-to-noise ratio (SNR) = 18 dB is used to emulate the fiber link. When the baud rate is higher than the sampling rate of DAC, the BER performance of conventional DFT-spread QPSK-OFDM is very poor as part of conventional DFT spread is not robust to brick-wall filter effect–induced ISI. However, the BER performance is better when FTN DFT-spread QPSK-OFDM signal is transmitted, as less proportion of power of signal is filtered out with brick-wall filter in frequency spectrum compression. After that, we prove MLSE decoding is more robust to resist ISI and can be used to further compensate the penalty induced by ISI. In this study, BER performance of single-channel 114 Gbaud and 126 Gbaud FTN DFT-spread QPSK-OFDM signal are measured and shown in **Figure 4A** and **Figure 4B**, respectively. We realize pre-equalization to resist bandwidth limitation induced ISI to some extent. Single-channel 114 Gbaud FTN DFT-spread QPSK-OFDM optical spectrums (0.02 nm) with and without pre-equalization are inserted in **Figure 2A**. The electrical spectrums of 114 Gbaud FTN-DFT-spread QPSK-OFDM optical spectrums with and without pre-equalization are inserted in **Figure 2B** and **Figure 2C**, respectively. After pre-equalization, BER performance of both 114 Gbaud and 126 Gbaud FTN DFT-spread QPSK-OFDM can be improved significantly, and MLSE decoding is also proved to be effective to resist ISI. Insets i) and ii) in **Figure 4A** show the constellations of 114 Gbaud FTN DFT-spread QPSK-OFDM with and without pre-equalization with OSNR at 30.4-dB, and insets i) and ii) in **Figure 4B** show the constellations of 126 Gbaud FTN DFT-spread QPSK-OFDM with and without pre-equalization with OSNR at 29.4-dB.

Figure 4C shows the measured BER versus input power per channel of the 3rd sub-channel of WDM after 420-km transmission. We measure the optimal input power per channel of all channels to be 0 dBm. It is easy to explain because high-power signals into the fiber will lead to chromatic dispersion and the nonlinear effect, which can

damage signal quality. If the input fiber power is too low, the signal-to-noise ratio will be low, and the noise will also affect the transmission quality of the signal. There is supposed to be a compromised power that makes the system perform optimally. The optimal input power of the other seven sub-channels is also measured to be 0 dBm.

Figure 4D shows the measured BER versus optical signal-to-noise ratio (OSNR) of the 3rd sub-channel of WDM in optical back-to-back (OBTB) and after 420-km fiber transmission. We observe no OSNR penalty compared to single-channel transmission. And negligible OSNR is observed after 420-km SMF transmission. After 420-km SMF transmission, the required OSNRs for 114 and 126 Gbaud FTN-DFT-spread QPSK-OFDM to achieve hard decision forward error correction (HD-FEC) threshold (3.8×10^{-3}) and SD-FEC threshold (2.4×10^{-2}) are 24.8 and 25.5 dB, respectively. Both the effective data rates of 114 and 126 Gbaud FTN-DFT-spread QPSK-OFDM are larger than 400 Gbit/s after removing overheads which includes TSs, CP, and corresponding FEC overheads. Insets i) and ii) in **Figure 4E** show the constellations of 114 and 126 Gbaud FTN DFT-spread QPSK-OFDM in WDM case with OSNR at 27.4-dB.

For all sub-channels 114 and 126 Gbaud FTN DFT-spread QPSK-OFDM, the measured BERs after 420-km SMF transmission shown in **Figure 4** are below 3.8×10^{-3} and 2.4×10^{-2}, respectively. Optical spectrum (0.02 nm) of WDM signal after 420-km transmission is inset in **Figure 4F**. While the computational complexity of SD-FEC is significantly higher, it is practical to transmit 114 Gbaud FTN-DFT-spread QPSK-OFDM to realize 400G services per wavelength for metro and regional applications.

CONCLUSION

In this study, for the first time we realize 400G FTN-DFT-spread QPSK-OFDM signal transmission per optical carrier for metro and regional applications. With the aid of DAF-based spectrum shaping and MLSE decoding in the receiver, we successfully transmit 8×400 Gbit/s FTN-DFT-spread QPSK-OFDM signal generated from 88 Gsa/s sampling rate DAC over 420 km SMF with the BER under 2.4×10^{-2}.

DATA AVAILABILITY STATEMENT

The raw data supporting the conclusion of this article will be made available by the authors, without undue reservation.

AUTHOR CONTRIBUTIONS

FL supervised the project and proposed the idea. PL wrote the article and did the experiment. HC did the simulation and discussed the results. WN drew the figures and analyzed the data.

FUNDING

This work is partly supported by the State Key Laboratory of Computer Architecture (ICT, CAS) under Grant (No. CARCH201907); Guangdong Basic and Applied Basic Research Foundation under Grant (Nos. 2019A1515110284, 2021A1515011962); Fundamental and Applied Basic Research Project of Guangzhou City under Grant (No. 202002030326).

REFERENCES

1. Zhang J, Yu J, and Chi N. Generation and Transmission of 512-Gb/s Quad-Carrier Digital Super-nyquist Spectral Shaped Signal. *Opt Express* (2013) 21(25):31212. doi:10.1364/OE.21.031212
2. Jia Z, Yu J, Chien H-C, Dong Z, and Di Huo D. Field Transmission of 100 G and Beyond: Multiple Baud Rates and Mixed Line Rates Using Nyquist-WDM Technology. *J Lightwave Technol* (2012) 30(24):3793–804. doi:10.1109/JLT.2012.2207373
3. Cai JX, Davidson CR, Lucero A, Zhang H, Foursa DG, Sinkin OV, et al. 20 Tbit/s Transmission over 6860 Km with Sub-nyquist Channel Spacing. *J lightwave Technol* (2011) 30(4):651–7.
4. Chien HC, Yu J, Jia Z, Dong Z, and Xiao X. 512-Gb/s Quad-Carrier PM-QPSK Transmission over 2400-km SMF-28 Subject to Narrowing 100-GHz Optical Bandwidth. In: 2012 38th European Conference and Exhibition on Optical Communications; 2012 Sept 16–20; Amsterdam, Netherlands. IEEE (2012). p. 1–3.
5. Zhang J, Yu J, Jia Z, and Chien H-C. 400 G Transmission of Super-nyquist-filtered Signal Based on Single-Carrier 110-GBaud PDM QPSK with 100-GHz Grid. *J Lightwave Technol* (2014) 32(19):3239–46. doi:10.1109/jlt.2014.2343016
6. Jia Z, Cai Y, Chien H-C, and Yu J. Performance Comparison of Spectrum-Narrowing Equalizations with Maximum Likelihood Sequence Estimation and Soft-Decision Output. *Opt Express* (2014) 22(5):6047. doi:10.1364/OE.22.006047
7. Zhang J, Huang B, and Li X. Improved Quadrature Duobinary System Performance Using Multi-Modulus Equalization. *IEEE Photon Technol Lett* (2013) 25(16):1630–3. doi:10.1109/lpt.2013.2273034
8. Zhang J, Yu J, Dong Z, Jia Z, Chien HC, Cai Y, et al. Transmission of 20× 440-Gb/s Super-nyquist-filtered Signals over 3600 Km Based on Single-Carrier 110-GBaud PDM QPSK with 100-GHz Grid. In *OFC 2014*. San Francisco, CA: IEEE (2014). p. 1–3.
9. Yu J, Zhang J, Dong Z, Jia Z, Chien H-C, Cai Y, et al. Transmission of 8×480-Gb/s Super-nyquist-filtering 9-QAM-like Signal at 100 GHz-Grid over 5000-km SMF-28 and Twenty-Five 100 GHz-Grid ROADMs. *Opt Express* (2013) 21(13):15686–91. doi:10.1364/oe.21.015686
10. Lu Y, Yu Y, Liu L, Huang Y, Wang X, and Li L. Faster-Than-Nyquist Signal Generation of Single Carrier 483-Gb/s (120.75-GBaud) PDM-QPSK with 92-GSa/s DAC. In: Optical Fiber Communication Conference. Los Angeles, CA: Optical Society of America (2017). p. W2A–44.
11. Zhu C, Corcoran B, Morshed M, Zhuang L, and Lowery AJ. Faster-Than-Nyquist DFT-S-OFDM Using Overlapping Sub-bands and Duobinary Filtering. In: Optical Fiber Communication Conference. Los Angeles, CA: Optical Society of America (2015). p. Th3G–5. doi:10.1364/ofc.2015.th3g.5
12. Li F, Li X, and Yu J. Performance Comparison of DFT-Spread and Pre-equalization for 8× 244.2-Gb/s PDM-16qam-OFDM. *J Lightwave Tech* (2014) 33(1):227–33. doi:10.1109/JLT.2014.2375794
13. Li F, Li X, Yu J, Chen L, and Yu C. Optimization of Training Sequence for DFT-Spread DMT Signal in Optical Access Network with Direct Detection Utilizing DML. *Opt Express* (2014) 22(19):22962. doi:10.1364/OE.22.022962
14. Li J, Tipsuwannakul E, Eriksson T, Karlsson M, and Andrekson PA. Approaching Nyquist Limit in WDM Systems by Low-Complexity Receiver-Side Duobinary Shaping. *J Lightwave Technol* (2012) 30(11):1664–76. doi:10.1109/jlt.2012.2190972

15. Chien H-C, Yu J, Jia Z, Dong Z, and Xiao X. Performance Assessment of Noise-Suppressed Nyquist-WDM for Terabit Superchannel Transmission. *J Lightwave Technol* (2012) 30(24):3965–71. doi:10.1109/jlt.2012.2207430
16. Zhang J, Chien HC, Xia Y, Chen Y, and Xiao J. A Novel Adaptive Digital Pre-equalization Scheme for Bandwidth Limited Optical Coherent System with DAC for Signal Generation. In: *OFC*. IEEE (2014). p. 1–3.
17. Ding L, Zou D, Wang W, Li F, and Li Z. Generation of faster-Than-Nyquist Coherent Optical DFT-Spread OFDM Signals with High-Baud and High-Order Modulations. *Opt Fiber Tech* (2021) 64:102526. doi:10.1016/J.YOFTE.2021.102526
18. Shankar H. *Duobinary Modulation for Optical Systems*. Santa Clara, CA: Inphi corporation (2002).
19. Xu X, Zhou E, Liu GN, Zuo T, Zhong Q, Zhang L, et al. Advanced Modulation Formats for 400-Gbps Short-Reach Optical Inter-connection. *Opt Express* (2015) 23(1):492–500. doi:10.1364/oe.23.000492
20. Xiao X, Li F, Yu J, Li X, Xia Y, and Chen F. 100-Gb/s Single-Band Real-Time Coherent Optical DP-16qam-OFDM Transmission and Reception. In: Optical Fiber Communication Conference. San Francisco, CA: Optical Society of America (2014). p. Th5C–6. doi:10.1364/ofc.2014.th5c.6

Conflict of Interest: The authors declare that the research was conducted in the absence of any commercial or financial relationships that could be construed as a potential conflict of interest.

Publisher's Note: All claims expressed in this article are solely those of the authors and do not necessarily represent those of their affiliated organizations, or those of the publisher, the editors and the reviewers. Any product that may be evaluated in this article, or claim that may be made by its manufacturer, is not guaranteed or endorsed by the publisher.